

Altered NK Cell Development and Enhanced NK Cell-Mediated Resistance to Mouse Cytomegalovirus in NKG2D-Deficient Mice

Zafirova, Biljana; Mandarić, Sanja; Antulov, Ronald; Krmpotić, Astrid; Jonsson, Helena; Yokoyama, Wayne M.; Jonjić, Stipan; Polić, Bojan

Source / Izvornik: *Immunity*, 2009, 31, 270 - 282

Journal article, Published version

Rad u časopisu, Objavljena verzija rada (izdavačev PDF)

<https://doi.org/10.1016/j.immuni.2009.06.017>

Permanent link / Trajna poveznica: <https://um.nsk.hr/um:nbn:hr:184:142440>

Rights / Prava: [Attribution-NonCommercial-NoDerivatives 4.0 International/Imenovanje-Nekomercijalno-Bez prerada 4.0 međunarodna](#)

Download date / Datum preuzimanja: **2025-03-24**



Repository / Repozitorij:

[Repository of the University of Rijeka, Faculty of Medicine - FMRI Repository](#)



Altered NK Cell Development and Enhanced NK Cell-Mediated Resistance to Mouse Cytomegalovirus in NKG2D-Deficient Mice

Biljana Zafirova,¹ Sanja Mandarić,^{1,3} Ronald Antulov,^{1,3} Astrid Krmpotić,¹ Helena Jonsson,² Wayne M. Yokoyama,² Stipan Jonjić,¹ and Bojan Polić^{1,*}

¹Department of Histology and Embryology, University of Rijeka School of Medicine, B. Branchetta 20, HR-51000 Rijeka, Croatia

²Howard Hughes Medical Institute, Rheumatology Division, Washington University Medical Centre, 660 S. Euclid Ave, Box 8045, St. Louis, MO 63110, USA

³These authors contributed equally to this work

*Correspondence: bojanp@medri.hr

DOI 10.1016/j.immuni.2009.06.017

SUMMARY

NKG2D is a potent activating receptor on natural killer (NK) cells and acts as a molecular sensor for stressed cells expressing NKG2D ligands such as infected or tumor-transformed cells. Although NKG2D is expressed on NK cell precursors, its role in NK cell development is not known. We have generated NKG2D-deficient mice by targeting the *Klrk1* locus. Here we provide evidence for an important regulatory role of NKG2D in the development of NK cells. The absence of NKG2D caused faster division of NK cells, perturbation in size of some NK cell subpopulations, and their augmented sensitivity to apoptosis. As expected, *Klrk1*^{-/-} NK cells are less responsive to tumor targets expressing NKG2D ligands. *Klrk1*^{-/-} mice, however, showed an enhanced NK cell-mediated resistance to mouse cytomegalovirus infection as a consequence of NK cell dysregulation. Altogether, these findings provide evidence for regulatory function of NKG2D in NK cell physiology.

INTRODUCTION

NKG2D is an activating receptor expressed on all mature natural killer (NK) cells and on NK precursors (NKPs) (Huntington et al., 2007b). NKG2D is also present on NKT cells, some $\gamma\delta$ T cells, and activated or memory $\alpha\beta$ T cells (Raulet, 2003; Saez-Borderias et al., 2006). Unlike other NKG2 molecules, NKG2D is a homodimer that recognizes mainly stress-induced major histocompatibility complex (MHC) class I-like ligands such as Rae-1 family (α , β , γ , δ , and ϵ), H60, and MULT-1 in mice, as well as MHC class I chain-related molecules (MICA or MICB) and UL16-binding proteins (ULBP1-4 or RAET1G) in humans (Bacon et al., 2004; Raulet, 2003). Thus, NKG2D receptor acts as a molecular sensor for stress-affected cells and can even override the inhibitory receptors engaged by MHC class I or MHC-class-I-like molecules.

NKG2D homodimer associates with two adaptor proteins with signaling properties, DAP10 and DAP12, which possess p85 phosphatidylinositol 3-kinase (PI3K)-binding YINM motif and

immunotyrosine-based activation motif (ITAM), respectively (Gilfillan et al., 2002; Wu et al., 2000; Wu et al., 1999). DAP10 activates PI3K, which is mainly responsible for cytotoxicity and survival of NK cells, as well as for costimulation of T cells, whereas DAP12 activates Src family kinases (ZAP70 and Syk), which are required for cytokine release and enhancement of cytotoxicity of NK cells. As a consequence of alternative NKG2D RNA splicing, there are two NKG2D isoforms, with shorter (NKG2D-S) and longer (NKG2D-L) intracellular domains. NKG2D-S is capable of binding both adaptor proteins, whereas NKG2D-L binds only DAP10 (Diefenbach et al., 2002; Gilfillan et al., 2002). Both isoforms are expressed in mouse, whereas only NKG2D-L exists in human NK cells.

The role of NKG2D in effector functions of the innate and adaptive immunity has been extensively studied in different experimental models. Various tumor cell lines expressing NKG2D ligands can activate NK or CD8⁺ T cells and induce their cytotoxicity in an NKG2D-dependent manner in vitro as well as in vivo (Bauer et al., 1999; Cerwenka et al., 2001; Diefenbach et al., 2001; Groh et al., 2001). NKG2D also senses cells expressing NKG2D ligands induced by the DNA-damage response pathway (Gasser et al., 2005). Thus, it is implicated in the control of tumor transformation as well as spontaneous tumor growth in vivo (Bartkova et al., 2005; Gorgoulis et al., 2005; Guerra et al., 2008).

The role of NKG2D was also shown in graft rejection (Ogasawara et al., 2005), autoimmunity (Ogasawara et al., 2004), and the control of virus infections and other intracellular pathogens (Cosman et al., 2001; Groh et al., 2001; Jonjić et al., 2008; Wiemann et al., 2005). To overcome NK cell activation via NKG2D, both mouse (MCMV) and human (HCMV) cytomegaloviruses encode proteins and/or microRNA aimed at downmodulation of the expression of cellular NKG2D ligands (Jonjić et al., 2008). Thus, MCMV appears to specifically target the NKG2D receptor, suggesting that NKG2D-mediated control is critical to modulating MCMV infections.

Any role for NKG2D in control of MCMV infections in C57BL/6 mice needs to account for the dominant role of *Klra8* (encoding Ly49H) in genetic resistance to MCMV. Ly49H couples to the ITAM-containing DAP12 signaling chain and is an activation receptor expressed only on NK cells (Lanier and Bakker, 2000). Consistent with this expression, depletion of NK cells confers enhanced susceptibility to MCMV. Moreover, in the absence of

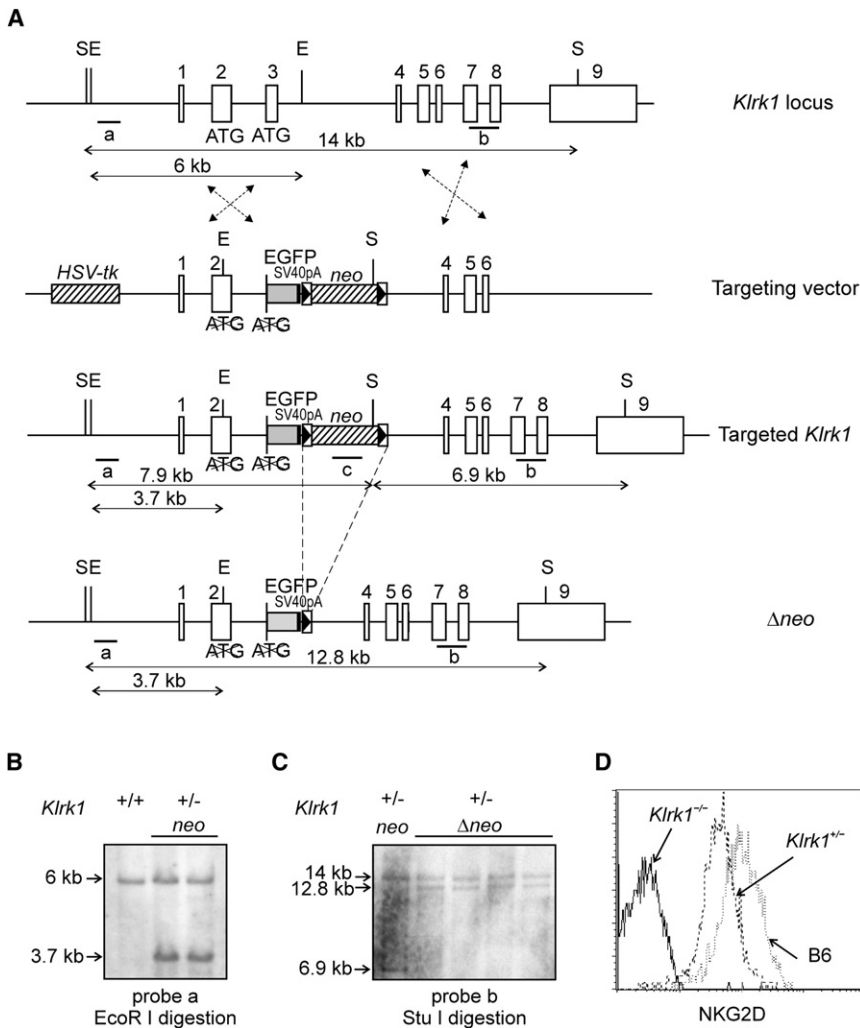


Figure 1. Generation of NKG2D-Deficient Mice

(A) Targeting of the *Klrk1* locus. Partial restriction map of the *Klrk1* locus with restriction sites for EcoR I (E) and Stu I (S) is shown. Selection markers (*HSV-tk* and *neo*), *loxP* sites (▶), external hybridization probes a and b, and internal probe c are depicted. The expected sizes of the DNA fragments are indicated above the lines.

(B and C) Southern-blot analyses of the targeted ES clones. (B) The homologous recombination as well as the introduced mutation in the second exon was tested by EcoR I digestion and external probe a. The DNA fragments of 3.7 and 6 kb represent targeted and WT NKG2D allele, respectively. (C) The Cre-mediated deletion of the *neo* cassette (Δneo) in the targeted ES clones (*neo*) was tested by the Stu I digestion and the external probe b. The DNA fragments of 12.8, 6.9, and 14 kb representing Δneo , *neo*, and WT alleles, respectively, are shown. (D) Flow-cytometric analysis of NKG2D expression on the spleen CD3 ϵ ⁻CD19⁻NK1.1⁺ NK cells of C57BL/6 (dotted line), *Klrk1*^{+/-} (dashed line), and *Klrk1*^{-/-} (line) is shown.

mice showed enhanced resistance to MCMV infection as a consequence of the observed NK cell dysregulation. During the infection, *Klrk1*^{-/-} NK cells mature faster, and a larger fraction of them are capable to exert their effector functions.

RESULTS

Targeting of the *Klrk1* Locus and Generation of *Klrk1*^{-/-} Mice

Targeting of the *Klrk1* locus was performed with the targeting vector contain-

ing the first six exons of the *Klrk1* gene and embryonic stem (ES) cells derived from C57BL/6 mice. In order to completely inactivate both NKG2D-L and NKG2D-S receptor variants, we mutated their leading ATGs in the coding sequence by introducing an EcoR I site in the second exon and an EGFP coding sequence with a transcriptional stop signal (SV40pA) followed by *loxP*-flanked neomycin resistance cassette (*neo*) in the third exon. The wild-type *Klrk1* locus and the locus upon homologous recombination of the targeting vector are depicted in Figure 1A. Cre-mediated deletion of the *neo* in the recombinant ES cells created the desired *Klrk1* allele (Figure 1A). Homologous recombinants were identified by Southern blotting (Figure 1B) and checked for random integration of the vector (data not shown) and for the deletion of the *neo* cassette upon transient Cre expression (Figure 1C). The mutated NKG2D allele was subsequently transmitted into the mouse germline, which was confirmed by polymerase chain reaction (PCR) and Southern blotting (data not shown).

The *Klrk1*^{-/-} mice bred normally and gave offspring according to the expected Mendelian ratio. Expression of NKG2D on NK cells isolated from the spleen of *Klrk1*^{-/-} mice was completely abolished (Figure 1D). In *Klrk1*^{+/-} mice, however, NKG2D was

expressing this receptor, we have developed a NKG2D-deficient mouse strain by targeting the *Klrk1* genetic locus (encoding NKG2D). Here we provide evidence that NKG2D plays an important regulatory role in the development, homeostasis, and survival of NK cells. NK cells in *Klrk1*^{-/-} mice proliferated faster, showed differential expression of several developmental markers, and exhibited augmented susceptibility to apoptosis, as compared to control mice. *Klrk1*^{-/-} NK cells were markedly less responsive to NKG2D-sensitive tumor targets, but they retained their reactivity when triggered by other activating receptors or cytokines. *Klrk1*^{-/-}

in the first six exons of the *Klrk1* gene and embryonic stem (ES) cells derived from C57BL/6 mice. In order to completely inactivate both NKG2D-L and NKG2D-S receptor variants, we mutated their leading ATGs in the coding sequence by introducing an EcoR I site in the second exon and an EGFP coding sequence with a transcriptional stop signal (SV40pA) followed by *loxP*-flanked neomycin resistance cassette (*neo*) in the third exon. The wild-type *Klrk1* locus and the locus upon homologous recombination of the targeting vector are depicted in Figure 1A. Cre-mediated deletion of the *neo* in the recombinant ES cells created the desired *Klrk1* allele (Figure 1A). Homologous recombinants were identified by Southern blotting (Figure 1B) and checked for random integration of the vector (data not shown) and for the deletion of the *neo* cassette upon transient Cre expression (Figure 1C). The mutated NKG2D allele was subsequently transmitted into the mouse germline, which was confirmed by polymerase chain reaction (PCR) and Southern blotting (data not shown).

The *Klrk1*^{-/-} mice bred normally and gave offspring according to the expected Mendelian ratio. Expression of NKG2D on NK cells isolated from the spleen of *Klrk1*^{-/-} mice was completely abolished (Figure 1D). In *Klrk1*^{+/-} mice, however, NKG2D was

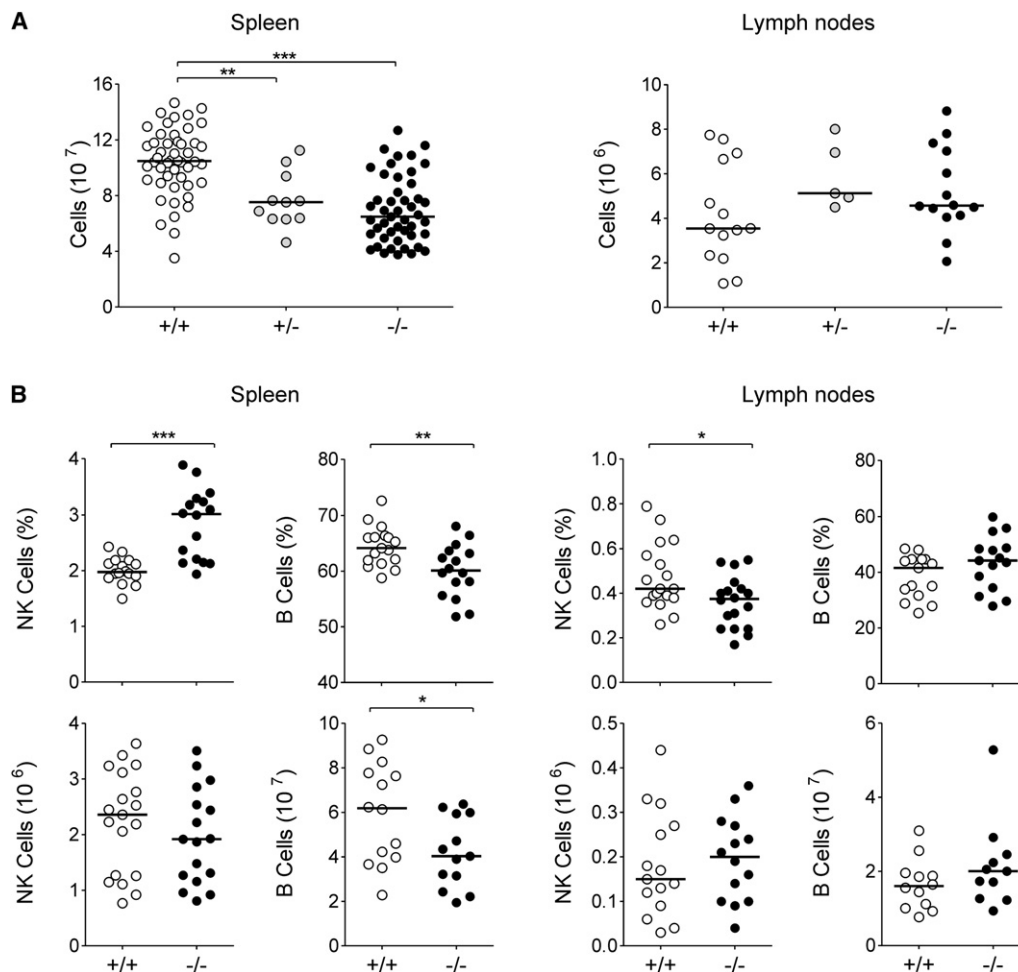


Figure 2. Reduced Cell Numbers in the Spleen of *Klrk1*^{-/-} Mice

(A) Cell numbers in the spleen and inguinal lymph nodes from 8–10-week-old C57BL/6, *Klrk1*^{+/-}, or *Klrk1*^{-/-} mice are shown.

(B) Percentages and absolute numbers of NK (CD3⁻CD19⁻NK1.1⁺) and B cells (CD19⁺) isolated from the spleen and inguinal lymph nodes of C57BL/6 and *Klrk1*^{-/-} mice are shown. Each symbol represents an individual mouse. Horizontal lines represent mean values. Statistically significant differences between the groups are indicated by asterisk symbols.

reduced in comparison to the C57BL/6 control. The expression of NKG2D ligands as well as MHC I molecules on mouse-derived embryonic fibroblasts (MEFs) was comparable between *Klrk1*^{-/-} and C57BL/6 mice, as confirmed by specific mAb and NKG2D tetramer staining (data not shown). Unfortunately, we have not observed any of the expected expression of EGFP in NK cells carrying the knock-in allele. By sequence analysis of the targeting vector, we subsequently found that the Kozak sequence at the leading ATG of the EGFP coding sequence was deleted during the subcloning procedure.

Reduced Number of Cells in the Spleen of *Klrk1*^{-/-} Mice

First we analyzed lymphocyte populations in the spleen and inguinal lymph nodes of the mutant and control mice to see whether the absence of NKG2D causes any abnormalities. We noticed that the spleen of adult *Klrk1*^{-/-} mice contained lower numbers of cells in comparison to the age-matched C57BL/6 control mice (Figure 2A). The observed cell loss was mainly

due to the reduced numbers of B and T cells (Figure 2B, Figure S1A available online) because population sizes of NK and NKT cells were comparable to the control (Figure 2B, Figure S1A). In contrast to the spleen, the numbers of total cells as well as of all lymphocyte populations (T, B, NK, and NKT) in inguinal lymph nodes were comparable to the control (Figure 2A, Figure S1A). Considering the reduced number of cells in the spleen, we also analyzed T and B cell development in *Klrk1*^{-/-} mice. We found no significant difference in total cell numbers or in the typical T and B cell subpopulations of the thymus and bone marrow, respectively (Figures S1C and S1D). Together, these results indicate that the reduction of T and B cells in the spleen, but not in the lymph nodes of *Klrk1*^{-/-} mice, is due to organ-specific differences in homeostasis.

NKG2D Plays a Role in NK Cell Development

Because NKG2D is expressed very early in the NK cell development (Huntington et al., 2007b), next we sought to test whether

the absence of this receptor influenced the development of NK cells. A set of markers characteristic for different developmental stages was used for the analysis of CD3 ϵ ⁻CD19⁻NK1.1⁺ NK cells from the bone marrow and spleen of 9-week-old *Klrk1*^{-/-} mice and their B6 littermates. A significant reduction of the NK cell population expressing c-Kit (CD117) in the bone marrow as well as in the spleen of *Klrk1*^{-/-} mice was observed (Figure 3A). In contrast, NK cell populations expressing CD127 and CD51 were at comparable frequency and slightly increased, respectively, in the bone marrow and present at reduced frequency in the spleen (Figure 3A). A similar pattern was also observed on 24-week-old littermates (Figure S2B).

We noticed that the reduction of c-Kit⁺ cells in the spleen (and to a lesser extent in the bone marrow) occurred mostly in the fraction of CD127⁻NK1.1⁺ ($p < 0.001$) or CD51⁻NK1.1⁺ ($p < 0.001$) NK cells (stages IV–V), whereas the fraction of CD127⁺NK1.1⁺ or CD51⁺NK1.1⁺ (stage III) c-Kit⁺ NK cells remained mostly unaffected (Figure 3B). In contrast, we observed a low percentage and no statistically significant difference in the c-Kit⁺ subpopulation of CD122⁺NK1.1⁻ NK cells (stage I) from the bone marrow and spleen, indicating that the reduction of c-Kit⁺ NK cells occurs in the transition from immature to mature NK cells rather than earlier (Figure 3B).

Other molecules that begin to be expressed at the immature stage (stages II–III), such as CD27, CD94, NKG2A, and most of the Ly49 family receptors (C, D, G2, H, and I), were expressed on NK cells in the bone marrow and spleen at amounts comparable to the control (Figure 3C, data not shown, Figure S2A). However, NK cells expressing Ly49A were significantly reduced in the bone marrow and the spleen (data not shown, Figure S2A). We also noticed a decrease of CD11b^{hi} and CD43^{hi} as well as Klr1⁺ populations of NK cells in the bone marrow but not in the spleen and liver, where they were at comparable sizes to the control (Figure 3C; Figure S3D). No difference in the frequency and absolute expression of activating (Ncr1, 2B4, and CD16) and inhibitory (NKPR1D) receptors on NK cells was observed (data not shown). In conclusion, the absence of NKG2D influences NK cell development, which is indicated by altered proportion of immature NK cells expressing c-Kit, CD51, and Ly49A, as well as mature cells expressing CD11b^{hi}, CD43^{hi}, and Klr1⁺.

Faster Division of NK Cells in *Klrk1*^{-/-} Mice

Considering the observed alterations of NK cell development in *Klrk1*^{-/-} mice, we sought to test the properties of *Klrk1*^{-/-} NK cells that might affect their developmental phenotype. First, we checked the proliferation dynamics of NK cells in vivo. *Klrk1*^{-/-} and control mice were pulsed with BrdU for 11 days and then checked for the decay of BrdU⁺ NK cells in the bone marrow and spleen at day 0, 15, and 21. Immediately after the pulse (day 0), a higher percentage of NK cells in the bone marrow of *Klrk1*^{-/-} mice (70.26% \pm 4.11%) was labeled in comparison to the control (60.52% \pm 3.72%), indicating their faster proliferation rate. This was not the case in the spleen (Figure 4A). However, the decay of BrdU⁺ NK cells was significantly faster in both bone marrow and spleen of *Klrk1*^{-/-} mice, indicating a different proliferation and/or apoptosis rate of these cells between the strains (Figure 4A). The calculated half-time of the decay in the bone marrow of *Klrk1*^{-/-} mice ($t_{1/2} = 10.84$ days) was approxi-

mately 50% shorter than in C57BL/6 mice ($t_{1/2} = 23.11$ days). In the spleen of both strains we observed longer decay half-times than in the bone marrow but similar difference between them (Figure 4A).

In order to see the contribution of different NK subsets to the BrdU labeling and decay, we also analyzed NK cells regarding the expression of c-Kit and CD11b. We looked at the expression of c-Kit versus CD11b on gated CD3⁻CD19⁻NK1.1⁺BrdU⁺ NK cells (Figure 4B) at day 0. Among the proliferating cells in the bone marrow of NKG2D-deficient mice, we observed the following: a larger population of c-Kit⁻CD11b^{lo} (stage II), a reduced population of c-Kit⁺CD11b^{lo} (stage III–IV), and comparable populations of c-Kit⁺CD11b^{hi} and c-Kit⁻CD11b^{hi} NK cells (stage V) to B6 control (Figure 4B). The differences observed in the bone marrow were much more pronounced in the spleen. There we found a robust increase of c-Kit⁻CD11b^{lo} NK cells (stage II) as well as the reduction of the c-Kit⁺CD11b^{lo} (stage III–IV) and c-Kit⁺CD11b^{hi} (stage V) populations of NK cells. The subpopulation of c-Kit⁻CD11b^{hi} NK cells (stage V) was at a comparable number with B6 control, as also seen in the bone marrow. Together, these data suggest that the reduction in the percentage of c-Kit⁺ NK cells in NKG2D-deficient mice is a consequence of a higher proliferation rate of immature NK cells (stage II) and/or faster differentiation and transition from the stage III to the more mature stage V accompanied by downmodulation of c-Kit.

Next we followed the BrdU decay dynamics of CD11b^{lo} and CD11b^{hi} NK cell subpopulations. The percentages of CD11b^{lo}BrdU⁺ and CD11b^{hi}BrdU⁺ out of total CD11b^{lo} and CD11b^{hi} NK cell subpopulations, respectively, were followed at indicated time points (Figure S3A). In the bone marrow of *Klrk1*^{-/-} mice, the decay half-time of less mature, CD11b^{lo} NK cells (Figure S3A) was shorter than in the control mice and very similar to the decay dynamics of total BrdU⁺ NK cells (Figure 4A). More mature CD11b^{hi} NK cells (Figure S3A) had similar decay dynamics to CD11b^{lo} NK cells in *Klrk1*^{-/-} as well as in control mice. Note that a higher percentage of CD11b^{hi}*Klrk1*^{-/-} NK cells (63.7% \pm 7.29%) was initially BrdU labeled (day 0) in comparison to the control (48.26% \pm 3.52%), indicating faster proliferation and transition from the less mature to the more mature NK cell compartment during the pulse period. The situation in the spleen was quite similar for the CD11b^{lo} subpopulation of NK cells to that described for the bone marrow (Figure S3A). Within the fraction of CD11b^{hi} NK cells (Figure S3A), we observed more pronounced difference (over 3-fold) in the decay half-times between the groups, which was mostly due to the slower decay of these cells in control mice.

Because we observed faster decay of BrdU-labeled NK cells, next we tested whether a differential susceptibility to apoptosis may explain, at least partially, this finding. NK cells were cultured either without treatment or with addition of rIL-15 (0.5 or 5 ng/ml) or rIL-2 (1000 U/ml), and apoptotic cells were determined upon 14 hr of culture by Annexin V staining. As shown in Figure 4C, higher susceptibility of *Klrk1*^{-/-} NK cells to apoptosis in comparison to the control was observed. IL-15 (Figure 4C) or IL-2 (data not shown) prevented to some extent apoptosis in both types of cells, but a significant difference between them in the susceptibility to apoptosis remained. Thus, *Klrk1*^{-/-} NK cells are more susceptible to apoptosis and at the same time more resistant

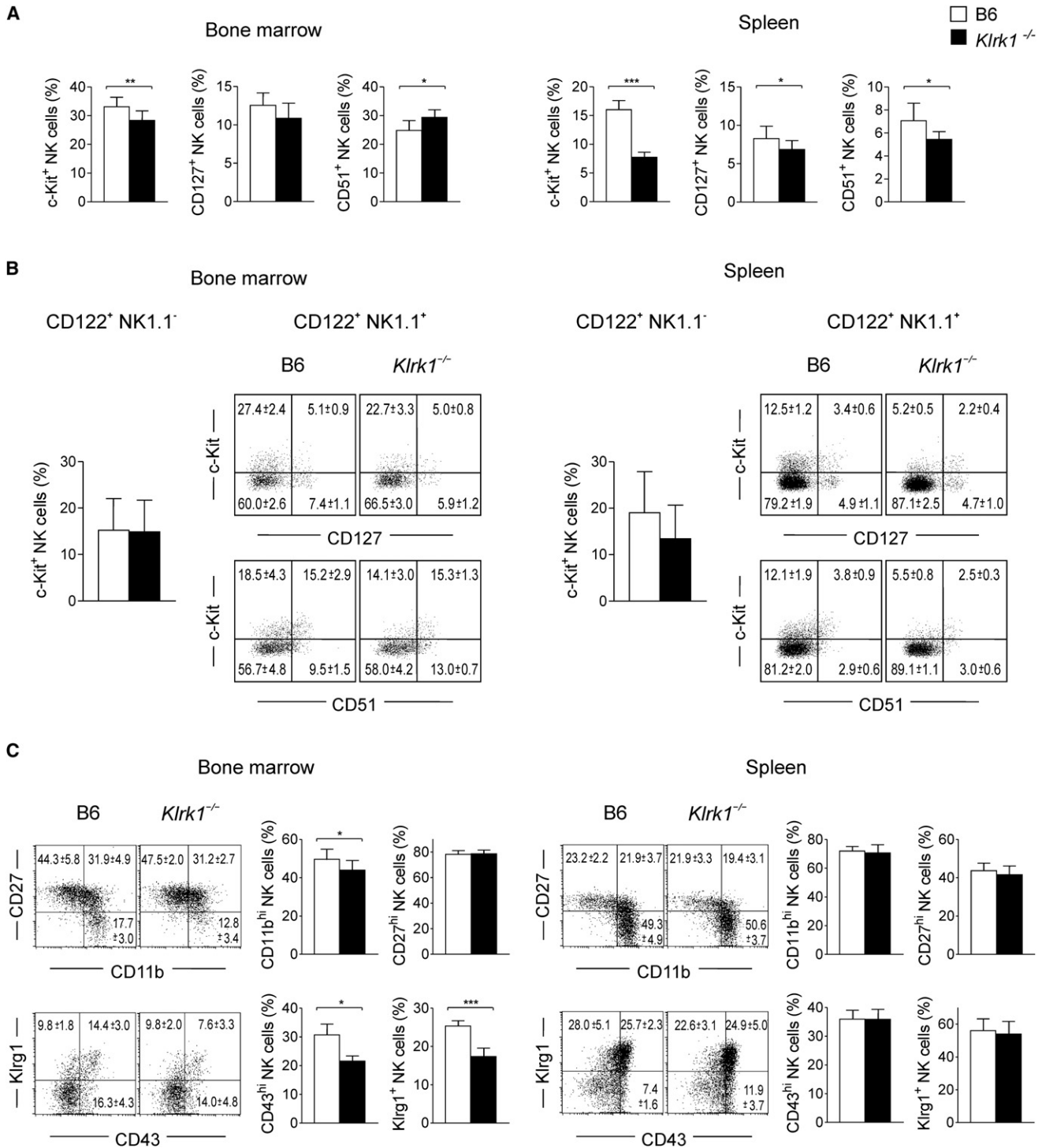


Figure 3. Altered NK Cell Development in *Klrk1*^{-/-} Mice

Analysis of NK cell subsets in the bone marrow and spleen of 9-week-old *Klrk1*^{-/-} mice and their B6 littermates.

(A) Comparison of c-Kit⁺, CD127⁺, and CD51⁺ subpopulations of CD3 ϵ ⁻CD19⁻NK1.1⁺ NK cells in the bone marrow and spleen.

(B) The representative dot-plot analyses of c-Kit, CD127, and CD51 expression on CD3 ϵ ⁻CD19⁻CD122⁺NK1.1⁺ NK cells are shown. Comparisons of c-Kit⁺ subpopulation of CD3 ϵ ⁻CD19⁻NK1.1⁻ NK cells in the bone marrow and spleen are shown (bar plots).

(C) Analyses of CD27, CD11b, CD43, and Klr1 expression on CD3 ϵ ⁻CD19⁻NK1.1⁺ NK cells are shown. Indicated numbers as well as bar plots (A, B, and C) represent mean percentages \pm standard deviation (SD) of individual data from four independent experiments (3–5 mice per group in each).

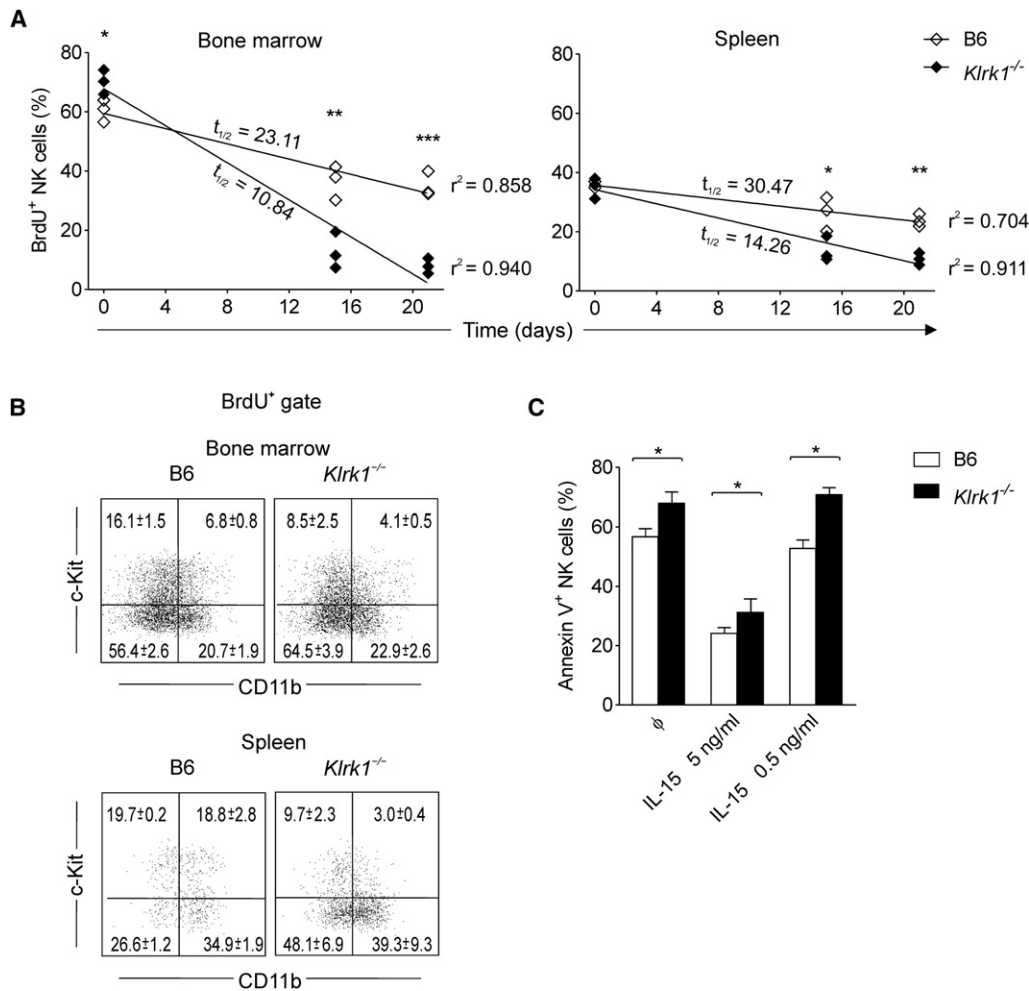


Figure 4. Faster Division of NK Cells in *Klrk1*^{-/-} Mice

(A and B) C57BL/6 (B6) and *Klrk1*^{-/-} mice were pulsed with BrdU in the drinking water for 11 days. (A) A decay of BrdU⁺ NK cells in the bone marrow and spleen at day 0, 15, and 21 is shown. Half-times ($t_{1/2}$) of the decay as well as goodness-of-fit (r^2) of the linear regressions are indicated. Representative of three independent experiments (3–4 mice per group in each) is shown. (B) Analyses of c-Kit and CD11b markers on BrdU⁺ NK subsets after 11 days of the BrdU treatment (day 0) are shown. Indicated numbers in dot plots represent mean percentages \pm SD of individual data. The analysis shown here is representative of three independent experiments (3–4 mice per group in each).

(C) Higher susceptibility of *Klrk1*^{-/-} NK cells to apoptosis. Freshly isolated cells from the spleen of C57BL/6 or *Klrk1*^{-/-} mice were cultured either without or with rIL-15 (0.5 or 5 ng/ml). Apoptotic cells were determined upon 14 hr of culture by Annexin V staining. Bars represent mean percentages \pm SD of individual data. The results shown here are representative of three independent experiments (3–5 mice per group in each).

to the IL-15-mediated rescue in comparison to the NKG2D-sufficient cells.

Klrk1^{-/-} NK Cells Are Less Responsive to Tumor Targets Expressing NKG2D Ligands

Next we sought to see how *Klrk1*^{-/-} NK cells respond to several tumor cell lines expressing NKG2D ligands. First we tested the capacity of *Klrk1*^{-/-} NK cells to kill tumor cell targets. NK cytotoxic assay was performed with NKG2D-sensitive and -resistant (RMA) tumor cells targets. As expected, *Klrk1*^{-/-} NK cells were less able to kill NKG2D-sensitive targets such as RMA-Rae1 δ or YAC1 than control *Klrk1*^{+/+} cells (Figure 5A). RMA cells were resistant to both NK cells tested (Figure 5A). We obtained also very similar results when we tested IFN- γ response of NK cells to the same tumor targets (Figure 5B). Thus, these results

confirmed that NKG2D signaling has an important role for the effector functions of NK cells.

We also tested whether *Klrk1*^{-/-} NK cells are able to recognize and kill MHC-class-I-deficient targets. RMA and RMA/S cells as targets were used in the analysis. As depicted in Figure S3B, *Klrk1*^{-/-} NK cells were equally efficient in the killing of MHC-class-I-negative RMA/S cells as compared to the control NK cells. Thus, NK cells in NKG2D-deficient mice are educated to recognize and respond to “missing self.”

Larger Fraction of *Klrk1*^{-/-} NK Cells Is Capable of Producing IFN- γ

Next we tested the ability of *Klrk1*^{-/-} NK cells to produce IFN- γ upon the activation with various stimuli. NK cells isolated from the spleen of *Klrk1*^{-/-} and C57BL/6 mice were subjected to

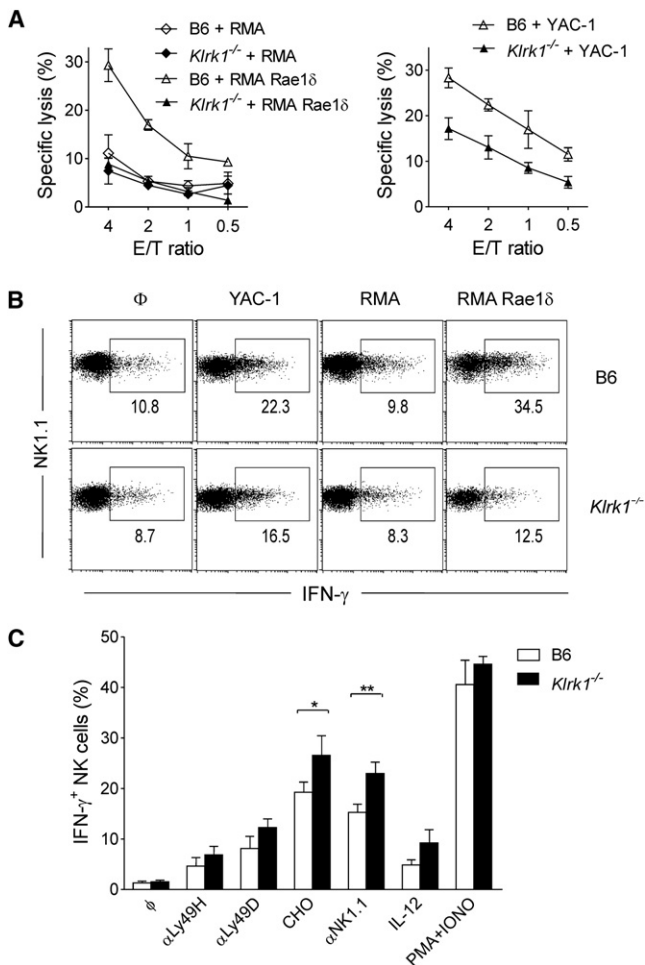


Figure 5. Functional Properties of *Klrk1*^{-/-} NK Cells

(A) NK cytotoxic assay. Equilibrated NK cells from the spleen of *Klrk1*^{-/-} and C57BL/6 mice were incubated with 10⁴ CFSE-labeled target cells for 4 hr at 37°C and in the presence of rIL-2 (1000 U/ml). Triplicates of samples for each effector to target (E:T) ratio were analyzed by flow cytometry. Values represent mean percentages ± SD of individual data. The results shown here are representative of three independent experiments (3–4 mice per group in each).

(B) NK cells from the spleen of *Klrk1*^{-/-} and C57BL/6 mice were incubated with the tumor cell targets in 1:1 ratio for 7 hr. The IFN-γ production was determined by the intracellular staining. Dot-plot analysis shown here is representative of three independent experiments (3 mice per group in each).

(C) NK cells were in vitro stimulated either by immobilized mAbs (αNK1.1, αLy49H, or αLy49D) or by incubation with CHO cell line, rIL-12, or PMA and Ionomycin. After an incubation period of 9 hr, intracellular IFN-γ was determined. When NK cells were stimulated with αNK1.1, they were stained with αDX5 mAb. Bars represent mean percentages ± SD of individual data. The analysis is representative of four independent experiments (3 mice per group in each).

crosslinking by immobilized mAbs to various activation receptors. Upon triggering of NK1.1, Ly49H, or Ly49D receptors, a somewhat larger fraction of *Klrk1*^{-/-} NK cells produced IFN-γ as compared to control NK cells (Figure 5C). Although these differences were variable in the series of experiments, the tendency for somewhat larger responses by *Klrk1*^{-/-} NK cells was consistently observed. We obtained similar results upon

the incubation of NK cells with Chinese hamster ovary (CHO) cell line (Figure 5C) expressing Ly49D ligands (Ildris et al., 1999), as well as after stimulation with IL-12 (Figure 5C). However, after either type of stimulation, we did not observe a difference in the quantity of IFN-γ production per cell between the tested NK cells (data not shown).

Enhanced NK Cell-Mediated Resistance to MCMV Infection in the *Klrk1*^{-/-} Mice

In our next experiments we sought to analyze the capacity of *Klrk1*^{-/-} NK cells to control MCMV infection in vivo. Because our mutant mice were on the C57BL/6 background, the mutant MCMV lacking *m157* gene (*Δm157*) had to be used. Namely, the resistance to MCMV of C57BL/6 is mainly due to the massive activation of NK cells via Ly49H receptors, which recognize MCMV *m157* gene product (Arase et al., 2002; Smith et al., 2002). Groups of *Klrk1*^{-/-}, *Klrk1*^{+/-}, and C57BL/6 mice (8–10 weeks old) were treated with PBS, αNK1.1, or αNKG2D prior to the intravenous infection. After 4 days, the mice were sacrificed and virus titers were determined in the spleen, liver, and lungs. Surprisingly, *Klrk1*^{-/-} mice were significantly better (liver and spleen, Figure 6A) or equal (lungs, data not shown) in the control of virus as compared to C57BL/6 mice. Similar results were obtained in independent experiments using 9-week-old mouse littermates as depicted in Figure S3C. In heterozygous mice, the virus titers in the spleen and liver were between the titers observed in the other two groups of mice, indicating that already lower amount of NKG2D expression (Figure 1D) in these mice positively influences the early immunosurveillance of the virus. Depletion of NK cells completely abrogated the observed effect, thus showing its NK cell dependency. As expected, neutralization of NKG2D had no effect on the virus control in all tested organs of *Klrk1*^{-/-} mice, whereas it had a slight or moderate effect in C57BL/6 mice. The question is whether one can interpret the inhibition of NKG2D by mAb (in C57BL/6 mice) in a similar way as NKG2D deficiency. One assumes that the injected antibody has the capacity to block NKG2D function to the same degree in every tissue, but this may not be the case. These differences may give rise to tissue-specific effects. On the other hand, our results indicate that the difference between the results obtained when comparing NKG2D-deficient mice and blocking of NKG2D in B6 mice by mAbs is a reflection of a higher responsiveness of NKG2D-deficient NK cells as a result of altered NK cell development (see above).

Because the less virulent tissue-culture-grown virus was used in the above experiment, next we tested the more virulent salivary gland isolate of wild-type MCMV (SGV). This virus preparation is particularly suitable to compare the capacity of *Klrk1*^{-/-} NK cells to resist the challenge by lethal doses of infectious virus. We observed higher resistance to the viral challenge (2 × 10⁵ plaque-forming units (PFUs) of SGV given intraperitoneally is equal to LD50 for C57BL/6 mice) of both *Klrk1*^{-/-} and *Klrk1*^{+/-} mice in comparison to the control mice, regardless of the *m157*-Ly49H interaction in this case. As shown on Figure 6B (left panel), the resistance to SGV infection was abolished by the depletion of NK cells. To test whether there is a subtle difference in resistance to SGV between the *Klrk1*^{-/-} and *Klrk1*^{+/-} mice, we challenged them with higher dose of the virus (3 × 10⁵ PFUs). In this experiment, we obtained clear separation in

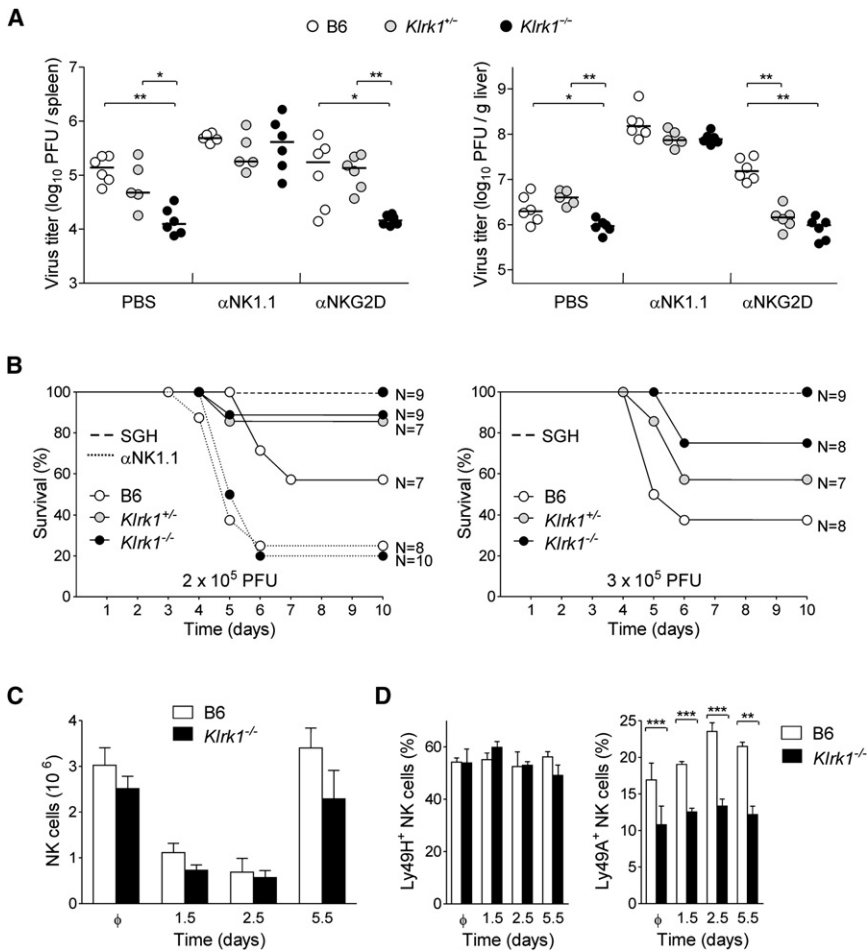


Figure 6. Enhanced Resistance of *Klrk1*^{-/-} Mice to MCMV Infection

(A) Groups of *Klrk1*^{-/-}, *Klrk1*^{+/-}, and C57BL/6 mice were treated with PBS, αNK1.1 (PK136), or αNKG2D (C7) prior to intravenous infection with 5 × 10⁵ PFU Δ*m157* MCMV. Virus titers determined in the spleen and liver 4 days after the infection are shown. Each symbol represents an individual mouse. Median values are indicated as horizontal lines. The results shown here are representative of six independent experiments.

(B) Survival of *Klrk1*^{-/-}, *Klrk1*^{+/-}, and C57BL/6 mice upon the infection with either 2 or 3 × 10⁵ PFU of SGV is shown. Control mice treated with mock-infected salivary gland homogenate (SGH, dashed line) as well as infected and NK cell depleted mice are shown (dotted line). Numbers of mice per group are indicated. Data are representative of three independent experiments.

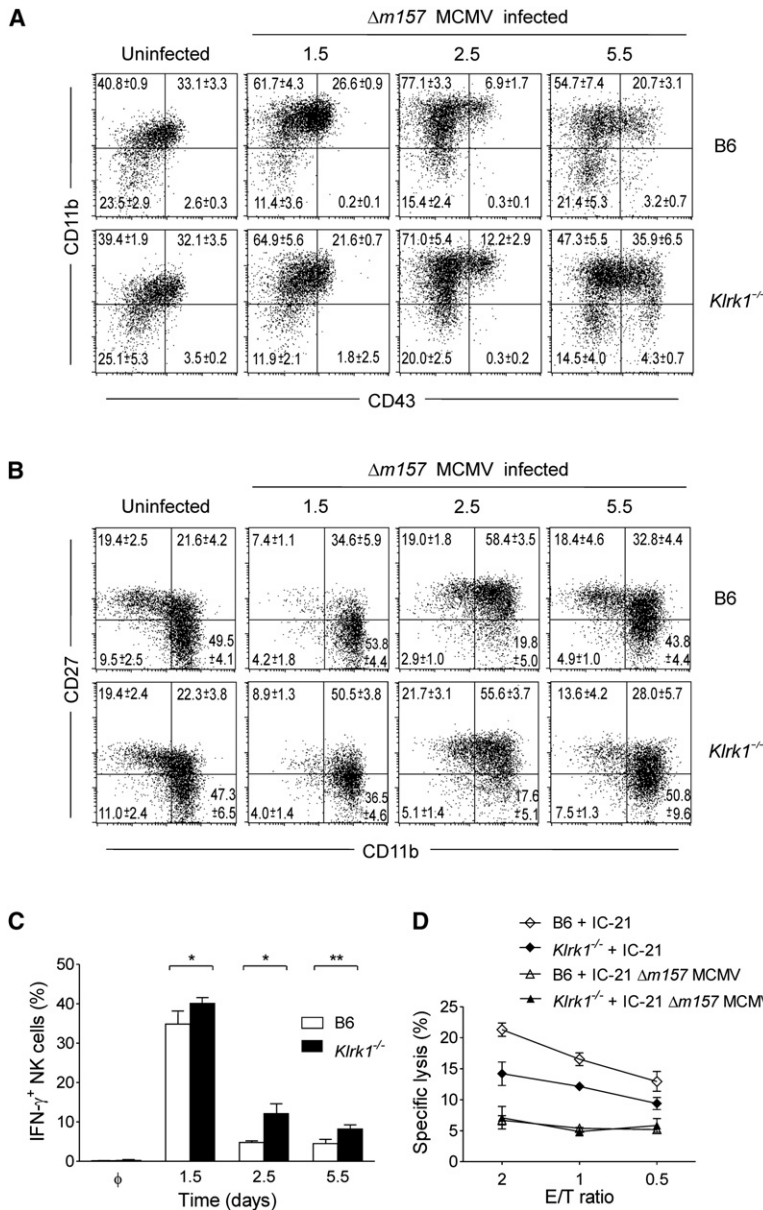
(C and D) Kinetics of NK cells in the spleen of *Klrk1*^{-/-} and C57BL/6 mice is shown (C). Percentages of Ly49H⁺ or Ly49A⁺ NK cell populations in the spleen of the Δ*m157* MCMV-infected mice are depicted for each indicated time point (D). Results (C and D) are expressed as mean ± SD of at least five mice per group. The results shown here (C and D) are representative of two independent experiments.

the resistance between all three groups of mice (Figure 6B, right panel). The *Klrk1*^{+/-} mice were more susceptible than *Klrk1*^{-/-} mice but also more resistant than the most susceptible C57BL/6 control.

Different Maturation Kinetics of *Klrk1*^{-/-} NK Cells during the MCMV Infection

Inasmuch as NKG2D deficiency alters the kinetics of development and decay of mature NK cells as well as the functional capacities (Figures 2–5, Figures S1–S3), we next sought to characterize surface markers and functional properties of peripheral *Klrk1*^{-/-} NK cells during the early course of MCMV infection. *Klrk1*^{-/-} and C57BL/6 mice were infected intravenously with Δ*m157* MCMV, and their NK cells were analyzed at day 1.5, 2.5, and 5.5 after the infection. First we looked at the absolute numbers of NK cells in the spleen, which dramatically decreased at day 1.5 after infection in both strains of mice (Figure 6C). The NK cell population started to recover between days 2.5 and 5.5 after infection with comparable kinetics between the infected mouse strains, following the pattern observed previously (Robbins et al., 2004). We then analyzed the expression of various NK cell markers at the indicated time points after the infection. The percentages of Ly49H⁺ NK cells did not change during the infection with Δ*m157* MCMV and were very similar in both mouse strains (Figure 6D). Also, we did not notice any significant differ-

ence of other activation markers, such as Ly49D, Ncr1, and CD16, between the strains, neither in the cell numbers or the expression amounts (data not shown). However, in the case of Ly49A, we noticed that the observed difference in size of Ly49A⁺ NK cell populations between the strains remained during the infection (Figure 6D). The analysis of CD11b and CD43 expression revealed different patterns in the maturation dynamics of NK cells between the strains (Figure 7A). At day 1.5 after infection, we found a decrease in the percentage of mature NK cell population (CD11b^{hi}CD43^{hi}) in wild-type (WT) and *Klrk1*^{-/-} mice. This effect was even more profound at day 2.5 after infection, particularly in the control mice. However, at day 5.5 after infection, we observed an increase of CD11b^{hi}CD43^{hi} NK cells in *Klrk1*^{-/-} mice in comparison to the C57BL/6 mice. We also analyzed NK cell subpopulations from spleen regarding the CD27 and CD11b expression (Figure 7B), markers for the maturity of peripheral NK cells (Hayakawa and Smyth, 2006). These data were consistent with the CD11b and CD43 staining. In the first phase of the infection (until day 2.5), we saw a dramatic decrease of immature R1 (CD27^{hi}CD11b^{lo}) population, as well as the most mature R3 (CD27^{lo}CD11b^{hi}) population, but an increase of mature R2 (CD27^{hi}CD11b^{hi}) population with slightly different dynamics between the strains. The decrease of R3 population was again faster in *Klrk1*^{-/-} mice. In the NK cell “recovery phase” (upon day 2.5 after infection), we also observed a faster increase of the R3 population in *Klrk1*^{-/-} mice (Figure 7B, right panel). Together, these data show faster maturation and/or migration dynamics of NK cells in MCMV-infected *Klrk1*^{-/-} mice in comparison to the control mice.



Larger Fraction of NK Cells in MCMV-Infected *Klrk1*^{-/-} Mice Produce IFN- γ

Next we addressed the capability of *Klrk1*^{-/-} NK cells to exert their effector functions during the infection. In the first series of experiments, we tested whether there are differences in the percentage of IFN- γ -producing NK cells in the spleen between the infected *Klrk1*^{-/-} and C57BL/6 mice. At the above-indicated time points, NK cells were briefly treated with rIL-2 and then tested for IFN- γ production by flow cytometry. As is depicted in Figure 7C, we observed a similar pattern in the percentage of IFN- γ -producing NK cells in both strains of mice, with the maximum at 1.5 days after infection. However, a larger fraction of NK cells from *Klrk1*^{-/-} mice produced IFN- γ at all tested time points during the infection as compared to the control. Consistent with the data described above, we did not observe any difference in the quantity of this production per cell.

Figure 7. The Maturation Kinetics and Functional Properties of *Klrk1*^{-/-} NK Cells during the MCMV Infection

(A and B) Analyses of (A) CD11b and CD43 and (B) CD27 and CD11b expression on the spleen NK cells at indicated days after infection with $\Delta m157$ MCMV. Representative dot plots of two independent experiments (3–4 mice per group in each) are depicted. Results are expressed as mean \pm SD. (C) Analysis of IFN- γ -producing NK cells isolated from *Klrk1*^{-/-} and C57BL/6 mice at indicated time points after the infection is shown. Freshly isolated spleen cells were incubated for 7 hr in the presence of rIL-2 (500 U/ml) and tested for IFN- γ production by intracellular staining. Bars represent mean percentages \pm SD of individual data. The analysis shown here is representative of three independent experiments (3–4 mice per group in each). (D) Results of NK cell killing of either uninfected or $\Delta m157$ MCMV-infected IC-21 cell targets are shown. The target cells were infected with 1 PFU/cell and incubated 14 hr before the staining. Triplicates of samples for each E:T ratio were analyzed by flow cytometry. Values represent mean percentages \pm SD. The results shown here are representative of three independent experiments.

Because the production of cytokines in NK cells is differently regulated than cytotoxicity, we also compared the capacity of *Klrk1*^{-/-} NK cells to kill MCMV-infected targets to the controls. Either uninfected or infected macrophage cell line IC-21 with wild-type (data not shown) or $\Delta m157$ MCMV (Figure 7D) was used as a target for NK cells. *Klrk1*^{-/-} NK cells were less efficient in killing uninfected IC-21 targets in comparison to the control, because of high expression of NKG2D ligands (data not shown), but they were equally inefficient as controls in killing infected IC-21 targets either with WT (data not shown) or with $\Delta m157$ MCMV (Figure 7D).

DISCUSSION

Here we provide evidence for a dual role of NKG2D in the physiology of NK cells: a regulatory role implicated in development, homeostasis, and survival, and another important for effector functions. In the absence of NKG2D, we observed faster division of NK cells, a perturbation in size of NK cell subpopulations, and augmented NK cell sensitivity to apoptosis. As expected, *Klrk1*^{-/-} NK cells were considerably less responsive to tumor cell targets expressing NKG2D ligands. However, *Klrk1*^{-/-} NK cells were more responsive to stimulation through other NK cell activation receptors, and *Klrk1*^{-/-} mice were more resistant to MCMV infection.

In another recently reported NKG2D-deficient mouse (Guerra et al., 2008), the authors did not observe major changes in the developmental subpopulations, and they did not study NK cell proliferation and apoptosis. It is difficult to reconcile the differences between the two studies. We both used embryonic stem cells derived from C57BL/6 mice, and in fact, we both used the same ES line, so strain differences seem unlikely to have caused any differences in our findings. Apart from different experimental

conditions, it is perhaps more likely that the Guerra et al. (2008) study was focused more on the importance of NKG2D deficiency in the immunosurveillance of tumors. Another possibility is that the differences are due to different targeting strategies, but this seems unlikely because most differences in targeting strategies are due to residual selectable markers, such as *neo*, that could affect neighboring genes. However, both groups deleted this segment from their mutant mice. Thus, only direct comparisons of both targeted mice with respect to development of NK cells could settle the question of whether or not these strains really differ.

Proliferation was enhanced within the immature and mature NK cell populations of the *Klrk1*^{-/-} mice. These changes include enhanced proliferation in stage II accompanied by a slight accumulation of these cells in the bone marrow, as well as the appearance of a larger fraction of functionally capable NK cells in the periphery. However, we did not observe accumulation of NK cells in the periphery, most likely because of the higher sensitivity of *Klrk1*^{-/-} NK cells to apoptosis. Thus, our data indicate a previously unknown regulatory role of NKG2D, which correlates with its appearance at the very early stages of NK cell development (Huntington et al., 2007b).

This regulatory function of NKG2D may operate in close connection with the IL-15R signaling pathway known to be essential for the development and survival of NK cells (Di Santo, 2006; Huntington et al., 2007a). A potential role for coupling of DAP10 with the IL-15R signaling pathway was recently described (Horng et al., 2007). The authors created a transgenic mouse model where DAP10 was fused with ubiquitin and, thus, subjected to degradation with consequent downmodulation of NKG2D. In this model, Stat5 was not phosphorylated and IL-15R signaling was largely abolished, causing a severe block in the development of NK cells. Jak3, as a part of the IL-15R signaling pathway (Jak3-Stat5), appeared to be an essential kinase for the phosphorylation of DAP10. In contrast, NK cells in the classical DAP10-deficient mice develop normally, which may now be ascribed to a redundancy in the signaling system as a result of the presence of intact NKG2D-DAP12 signaling complexes on the cell surface (Gilfillan et al., 2002). It has been shown that Syk can regulate cell survival and cytotoxicity of NK cells over PI3K (Jiang et al., 2002; Jiang et al., 2003). Similarly, DAP12 deficiency is also redundant and does not cause developmental defects of NK cells (Bakker et al., 2000; Tomasello et al., 2000). Because both signaling pathways, NKG2D and IL-15R, can activate PI3K, which is implicated in the control of proliferation, cytotoxicity, and resistance to apoptosis (Bonema et al., 1994; Horng et al., 2007; Jiang et al., 2000; Jiang et al., 2003; Zompi et al., 2003), the “unleashed” proliferation as well as augmented sensitivity to apoptosis of NK cells in our model may be due to a regulatory function of NKG2D controlling both pathways, where PI3K plays a central role. Recently, it has been reported that B cell adaptor for PI3K (BCAP), a cytosolic adaptor molecule that connects the phosphorylated YxxM motif on membrane receptors or adaptors with PI3K (Okada et al., 2000), also operates in NK cells (MacFarlane et al., 2008). Interestingly, BCAP-deficient mice featured somewhat slower proliferation of NK cells, increased NK cell numbers in the spleen, enhanced effector capabilities, and higher resistance to apoptosis (MacFarlane et al., 2008). In contrast, in transgenic

models with sustained NKG2D ligands expression like MICA (Wiemann et al., 2005) and Rae1 ϵ (Oppenheim et al., 2005), and consequent downregulation of NKG2D on NK cells, the above-discussed phenomenon was not reported, although this could be related to persistent NK cell stimulation and cross-tolerization of other activation receptors (Coudert et al., 2008).

As expected, we observed that *Klrk1*^{-/-} NK cells have markedly lower cytolytic and IFN- γ response to NKG2D-sensitive tumor targets. This finding is in accordance with the study done on a recently published NKG2D-deficient mouse (Guerra et al., 2008). Thus, the results from both of the NKG2D-deficient mice, as well as the data obtained from other models of NKG2D deficiency (Oppenheim et al., 2005; Wiemann et al., 2005), confirm important effector functions of NKG2D in the control of at least some tumors and infections in vivo.

The enhanced resistance of *Klrk1*^{-/-} mice to MCMV, however, was surprising considering the inability of mice to mount an NKG2D-dependent virus control because of the viral downmodulation of NKG2D ligands (Bubic et al., 2004; Jonjic et al., 2008). We expected less or, at most, equal NK cell-mediated control of the virus in *Klrk1*^{-/-} mice, particularly in the context of our recent observation that the mature form of Rae1 δ is rather resistant to the downmodulation (Arapovic et al., 2009). The reason for the enhanced resistance of *Klrk1*^{-/-} mice to MCMV could be a different quality of NK cell response triggered by other activation receptors or cytokines as a matter of the NK cell dysregulation. Proliferation of NK cells during the early phase of MCMV infection is promoted by IFN- α and IFN- β (Orange and Biron, 1996), which induces IL-15 (Nguyen et al., 2002). The presence of IL-15, either in soluble form or *trans*-presented by dendritic cells (Burkett et al., 2004; Lucas et al., 2007), can enhance NK cells proliferation and maturation, particularly in the absence of NKG2D as discussed above. Recent studies report specific and vigorous proliferation of Ly49H⁺ NK cells during the early MCMV infection, presumably because of their increased sensitivity to limited amounts of IL-15. This sensitivity was not a consequence of IL-15R upregulation, but rather of Ly49H-DAP12-mediated tuning of NK cells (French et al., 2006). It may well be that NKG2D regulates signaling of Ly49H as well as of other activation receptors, mediated through DAP10 and/or DAP12 adaptors, and thus controls proliferation and survival of NK cells, as discussed above. There is evidence for close cooperation of NKG2D and other activation receptors in terms of costimulation (Ho et al., 2002) as well as of cross-tolerization upon sustained engagement of NKG2D (Coudert et al., 2008). Secretion of cytokines like IL-12 and IL-18 during the early course of the infection could induce IFN- γ production in a larger fraction of the response-capable *Klrk1*^{-/-} NK cells. Therefore, we believe that the enhanced resistance of NKG2D-deficient mice to MCMV infection is mainly a consequence of NK cell dysregulation resulting in higher frequency of NK cells capable to respond.

EXPERIMENTAL PROCEDURES

Mice

C57BL/6, *Klrk1*^{+/-}, and *Klrk1*^{-/-} mice were maintained under specific pathogen-free (SPF) conditions at the Laboratory Mouse Breeding and Engineering Centre (LAMRI), University of Rijeka School of Medicine. All experiments were

approved by the Ethical Committee of the School of Medicine and conducted in accordance with the international guidelines for animal care and experimental use. Mice were analyzed at the age of 8–10 weeks, if not differently indicated.

Generation of NKG2D-Deficient Mice

Bruce 4 ES cells (C57BL/6) and feeder cells were grown under conditions described previously (Kuhn and Torres, 2002). The ES cells (10^7) were transfected with 30 μ g linearized (Not I) pNKG2D-EGFP1 vector (see Supplemental Experimental Procedures). After positive (G418) and negative (Gancyclovir) selection, ES cell clones were picked and screened for homologous recombinants by Southern blotting with the external 5' probe a. The internal probe c was used to exclude random integrations of the vector. For deletion of the *loxP*-flanked neo cassette in vitro, two selected clones were transiently transfected with pGK-Cre vector and screened for the deletion by Southern blotting. DNA from G418-sensitive colonies were digested with Stu I and hybridized with the external probe b. Two neo-deleted ES cell clones were injected into CB20 blastocysts, which were subsequently transferred into the uteri of F1 (BALB/c \times C57BL/6) foster mothers. From each injected clone we obtained several chimeras, which were crossed to C57BL/6 mice and given germline transmission of the mutated *Klrk1* allele. Mutants were crossed to C57BL/6 three times during the expansion before being maintained in homozygous breeding. Some experiments, as indicated, were performed on littermates of heterozygous breeding.

In Vivo BrdU Labeling and Detection

Klrk1^{-/-} and C57BL/6 mice were fed with drinking water containing 0.8 mg/ml BrdU (Sigma) for 11 days prior to the initial time point (day 0). At days 0, 14, and 21, NK cells were isolated from the spleen and bone marrow and stained for surface markers. After surface staining, the cells were fixed, permeabilized, and intracellularly labeled with the FITC BrdU Flow kit (BD) according to the manufacturer's instructions.

Apoptosis Assay

Freshly isolated splenocytes were cultured in complete RPMI 1640 supplemented with 10% FCS (R10) for 14 hr in the presence or absence of rIL-15 (0.5 or 5 ng/ml) or rIL-2 (1000 U/ml, BD). The cells were then stained by Annexin V-PE with Annexin V Apoptosis Kit (BD) according to the manufacturer's instructions.

MCMV Infection

The tissue-culture-grown $\Delta m157$ MCMV and the salivary gland isolate of wild-type MCMV (SGV) were produced and purified, as described previously (Brune et al., 2001). The mice were treated with α NK1.1⁺ (PK136, 300 μ g/mouse), α NKG2D (C7, 300 μ g/mouse), or PBS 24 hr before intravenous injection of 5×10^5 PFUs of $\Delta m157$ MCMV. Four days after the infection, the mice were sacrificed and viral titers were determined in various organs with the standard virus plaque assay (Bubic et al., 2004).

For determining the capacity of *Klrk1*^{-/-} NK cells to resist challenge infection with more virulent MCMV, the mice were infected with either 2 or 3 $\times 10^5$ PFUs of SGV intraperitoneally. The control groups of mice were treated with the same amount of salivary gland homogenate isolated from the mock-infected mice. The mice were treated with either α NK1.1 or PBS 24 hr prior to the infection. Survival of the mice was monitored during the period of 30 days after the infection.

Statistics

Statistical significance was calculated by unpaired two-tailed Student's *t* test with Prism4 software (GraphPad Software). The significant differences between tested groups are indicated with symbols as follows: $p < 0.05$ (*), $p < 0.01$ (**), and $p < 0.001$ (***). Statistical analyses of the virus titers were done with the Mann-Whitney *U* test.

SUPPLEMENTAL DATA

Supplemental Data include Supplemental Experimental Procedures and three figures and can be found with this article online at [http://www.cell.com/immunity/supplemental/S1074-7613\(09\)00315-X](http://www.cell.com/immunity/supplemental/S1074-7613(09)00315-X).

ACKNOWLEDGMENTS

We thank A. Steinle and A. Diefenbach for critical reading of the manuscript and comments as well as J. Arapovic for helpful discussions. We especially express our gratitude to S. Slavic Stupac for excellent technical assistance and to M. Samsa for animal care. We also thank C. Uthoff-Hachenberg and D. Rumora for technical advice and help. This work was supported by the Croatian Ministry of Science, Education and Sport (grants TP01/006201 (103), 0062005, and 062-0621261-1271, as well as a Croatian-Israeli grant to B.P.).

Received: August 5, 2008

Revised: March 17, 2009

Accepted: June 1, 2009

Published online: July 23, 2009

REFERENCES

- Arapovic, J., Lenac, T., Antulov, R., Polic, B., Ruzsics, Z., Carayannopoulos, L.N., Koszinowski, U.H., Krmpotic, A., and Jonjic, S. (2009). Differential susceptibility of RAE-1 isoforms to mouse cytomegalovirus. *J. Vir.* Published online June 3, 2009. 10.1128/JVI.02549-08.
- Arase, H., Mocarski, E.S., Campbell, A.E., Hill, A.B., and Lanier, L.L. (2002). Direct recognition of cytomegalovirus by activating and inhibitory NK cell receptors. *Science* 296, 1323–1326.
- Bacon, L., Eagle, R.A., Meyer, M., Easom, N., Young, N.T., and Trowsdale, J. (2004). Two human ULBP/RAET1 molecules with transmembrane regions are ligands for NKG2D. *J. Immunol.* 173, 1078–1084.
- Bakker, A.B., Hoek, R.M., Cerwenka, A., Blom, B., Lucian, L., McNeil, T., Murray, R., Phillips, L.H., Sedgwick, J.D., and Lanier, L.L. (2000). DAP12-deficient mice fail to develop autoimmunity due to impaired antigen priming. *Immunity* 13, 345–353.
- Bartkova, J., Horejsi, Z., Koed, K., Kramer, A., Tort, F., Zieger, K., Guldborg, P., Sehested, M., Nesland, J.M., Lukas, C., et al. (2005). DNA damage response as a candidate anti-cancer barrier in early human tumorigenesis. *Nature* 434, 864–870.
- Bauer, S., Groh, V., Wu, J., Steinle, A., Phillips, J.H., Lanier, L.L., and Spies, T. (1999). Activation of NK cells and T cells by NKG2D, a receptor for stress-inducible MICA. *Science* 285, 727–729.
- Bonnema, J.D., Karnitz, L.M., Schoon, R.A., Abraham, R.T., and Leibson, P.J. (1994). Fc receptor stimulation of phosphatidylinositol 3-kinase in natural killer cells is associated with protein kinase C-independent granule release and cell-mediated cytotoxicity. *J. Exp. Med.* 180, 1427–1435.
- Brown, M.G., Dokun, A.O., Heusel, J.W., Smith, H.R., Beckman, D.L., Blattenberger, E.A., Dubbelde, C.E., Stone, L.R., Scalzo, A.A., and Yokoyama, W.M. (2001). Vital involvement of a natural killer cell activation receptor in resistance to viral infection. *Science* 292, 934–937.
- Brune, W., Hengel, H., and Koszinowski, U.H. (2001). A mouse model for cytomegalovirus infection. In *Current Protocols in Immunology*, J.E. Coligan, et al., eds. (Hoboken, NJ: John Wiley & Sons), pp. 1–13.
- Bubic, I., Wagner, M., Krmpotic, A., Sauljic, T., Kim, S., Yokoyama, W.M., Jonjic, S., and Koszinowski, U.H. (2004). Gain of virulence caused by loss of a gene in murine cytomegalovirus. *J. Virol.* 78, 7536–7544.
- Burkett, P.R., Koka, R., Chien, M., Chai, S., Boone, D.L., and Ma, A. (2004). Coordinate expression and trans presentation of interleukin (IL)-15Ralpha and IL-15 supports natural killer cell and memory CD8+ T cell homeostasis. *J. Exp. Med.* 200, 825–834.
- Cerwenka, A., Baron, J.L., and Lanier, L.L. (2001). Ectopic expression of retinoic acid early inducible-1 gene (RAE-1) permits natural killer cell-mediated rejection of a MHC class I-bearing tumor in vivo. *Proc. Natl. Acad. Sci. USA* 98, 11521–11526.
- Cosman, D., Mullberg, J., Sutherland, C.L., Chin, W., Armitage, R., Fanslow, W., Kubin, M., and Chalupny, N.J. (2001). ULBPs, novel MHC class I-related molecules, bind to CMV glycoprotein UL16 and stimulate NK cytotoxicity through the NKG2D receptor. *Immunity* 14, 123–133.

- Coudert, J.D., Scarpellino, L., Gros, F., Vivier, E., and Held, W. (2008). Sustained NKG2D engagement induces cross-tolerance of multiple distinct NK cell activation pathways. *Blood* *111*, 3571–3578.
- Daniels, K.A., Devora, G., Lai, W.C., O'Donnell, C.L., Bennett, M., and Welsh, R.M. (2001). Murine cytomegalovirus is regulated by a discrete subset of natural killer cells reactive with monoclonal antibody to Ly49H. *J. Exp. Med.* *194*, 29–44.
- Diefenbach, A., Jensen, E.R., Jamieson, A.M., and Raulet, D.H. (2001). Rae1 and H60 ligands of the NKG2D receptor stimulate tumour immunity. *Nature* *413*, 165–171.
- Diefenbach, A., Tomasello, E., Lucas, M., Jamieson, A.M., Hsia, J.K., Vivier, E., and Raulet, D.H. (2002). Selective associations with signaling proteins determine stimulatory versus costimulatory activity of NKG2D. *Nat. Immunol.* *3*, 1142–1149.
- Di Santo, J.P. (2006). Natural killer cell developmental pathways: A question of balance. *Annu. Rev. Immunol.* *24*, 257–286.
- French, A.R., Sjolín, H., Kim, S., Koka, R., Yang, L., Young, D.A., Cerboni, C., Tomasello, E., Ma, A., Vivier, E., et al. (2006). DAP12 signaling directly augments proliferative cytokine stimulation of NK cells during viral infections. *J. Immunol.* *177*, 4981–4990.
- Gasser, S., Orsulic, S., Brown, E.J., and Raulet, D.H. (2005). The DNA damage pathway regulates innate immune system ligands of the NKG2D receptor. *Nature* *436*, 1186–1190.
- Giffillan, S., Ho, E.L., Cella, M., Yokoyama, W.M., and Colonna, M. (2002). NKG2D recruits two distinct adaptors to trigger NK cell activation and costimulation. *Nat. Immunol.* *3*, 1150–1155.
- Gorgoulis, V.G., Vassiliou, L.V., Karakaidos, P., Zacharatos, P., Kotsinas, A., Liloglou, T., Venere, M., Dittullo, R.A., Jr., Kastrinakis, N.G., Levy, B., et al. (2005). Activation of the DNA damage checkpoint and genomic instability in human precancerous lesions. *Nature* *434*, 907–913.
- Groh, V., Rhinehart, R., Randolph-Habecker, J., Topp, M.S., Riddell, S.R., and Spies, T. (2001). Costimulation of CD8 α T cells by NKG2D via engagement by MIC induced on virus-infected cells. *Nat. Immunol.* *2*, 255–260.
- Guerra, N., Tan, Y.X., Joncker, N.T., Choy, A., Gallardo, F., Xiong, N., Knoblaugh, S., Cado, D., Greenberg, N.M., and Raulet, D.H. (2008). NKG2D-deficient mice are defective in tumor surveillance in models of spontaneous malignancy. *Immunity* *28*, 571–580.
- Hayakawa, Y., and Smyth, M.J. (2006). CD27 dissects mature NK cells into two subsets with distinct responsiveness and migratory capacity. *J. Immunol.* *176*, 1517–1524.
- Ho, E.L., Carayannopoulos, L.N., Poursine-Laurent, J., Kinder, J., Plougastel, B., Smith, H.R., and Yokoyama, W.M. (2002). Costimulation of multiple NK cell activation receptors by NKG2D. *J. Immunol.* *169*, 3667–3675.
- Hornig, T., Bezbradica, J.S., and Medzhitov, R. (2007). NKG2D signaling is coupled to the interleukin 15 receptor signaling pathway. *Nat. Immunol.* *8*, 1345–1352.
- Huntington, N.D., Puthalakath, H., Gunn, P., Naik, E., Michalak, E.M., Smyth, M.J., Tabarias, H., Degli-Esposti, M.A., Dewson, G., Willis, S.N., et al. (2007a). Interleukin 15-mediated survival of natural killer cells is determined by interactions among Bim, Noxa and Mcl-1. *Nat. Immunol.* *8*, 856–863.
- Huntington, N.D., Vosshenrich, C.A., and Di Santo, J.P. (2007b). Developmental pathways that generate natural-killer-cell diversity in mice and humans. *Nat. Rev. Immunol.* *7*, 703–714.
- Idris, A.H., Smith, H.R., Mason, L.H., Ortaldo, J.R., Scalzo, A.A., and Yokoyama, W.M. (1999). The natural killer gene complex genetic locus Chok encodes Ly-49D, a target recognition receptor that activates natural killing. *Proc. Natl. Acad. Sci. USA* *96*, 6330–6335.
- Jiang, K., Zhong, B., Gilvary, D.L., Corliss, B.C., Hong-Geller, E., Wei, S., and Djeu, J.Y. (2000). Pivotal role of phosphoinositide-3 kinase in regulation of cytotoxicity in natural killer cells. *Nat. Immunol.* *1*, 419–425.
- Jiang, K., Zhong, B., Gilvary, D.L., Corliss, B.C., Vivier, E., Hong-Geller, E., Wei, S., and Djeu, J.Y. (2002). Syk regulation of phosphoinositide 3-kinase-dependent NK cell function. *J. Immunol.* *168*, 3155–3164.
- Jiang, K., Zhong, B., Ritchey, C., Gilvary, D.L., Hong-Geller, E., Wei, S., and Djeu, J.Y. (2003). Regulation of Akt-dependent cell survival by Syk and Rac. *Blood* *101*, 236–244.
- Jonjic, S., Babic, M., Polic, B., and Krmpotic, A. (2008). Immune evasion of natural killer cells by viruses. *Curr. Opin. Immunol.* *20*, 30–38.
- Kuhn, R., and Torres, R.M. (2002). Cre/loxP recombination system and gene targeting. *Methods Mol. Biol.* *180*, 175–204.
- Lanier, L.L., and Bakker, A.B. (2000). The ITAM-bearing transmembrane adaptor DAP12 in lymphoid and myeloid cell function. *Immunol. Today* *21*, 611–614.
- Lee, S.H., Girard, S., Macina, D., Busa, M., Zafer, A., Belouchi, A., Gros, P., and Vidal, S.M. (2001). Susceptibility to mouse cytomegalovirus is associated with deletion of an activating natural killer cell receptor of the C-type lectin superfamily. *Nat. Genet.* *28*, 42–45.
- Lucas, M., Schachterle, W., Oberle, K., Aichele, P., and Diefenbach, A. (2007). Dendritic cells prime natural killer cells by trans-presenting interleukin 15. *Immunity* *26*, 503–517.
- MacFarlane, A.W., Yamazaki, T., Fang, M., Sigal, L.J., Kurosaki, T., and Campbell, K.S. (2008). Enhanced NK-cell development and function in BCAP-deficient mice. *Blood* *112*, 131–140.
- Nguyen, K.B., Salazar-Mather, T.P., Dalod, M.Y., Van Deusen, J.B., Wei, X.Q., Liew, F.Y., Caligiuri, M.A., Durbin, J.E., and Biron, C.A. (2002). Coordinated and distinct roles for IFN- α beta, IL-12, and IL-15 regulation of NK cell responses to viral infection. *J. Immunol.* *169*, 4279–4287.
- Ogasawara, K., Hamerman, J.A., Ehrlich, L.R., Bour-Jordan, H., Santamaria, P., Bluestone, J.A., and Lanier, L.L. (2004). NKG2D blockade prevents autoimmune diabetes in NOD mice. *Immunity* *20*, 757–767.
- Ogasawara, K., Benjamin, J., Takaki, R., Phillips, J.H., and Lanier, L.L. (2005). Function of NKG2D in natural killer cell-mediated rejection of mouse bone marrow grafts. *Nat. Immunol.* *6*, 938–945.
- Okada, T., Maeda, A., Iwamatsu, A., Gotoh, K., and Kurosaki, T. (2000). BCAP: The tyrosine kinase substrate that connects B cell receptor to phosphoinositide 3-kinase activation. *Immunity* *13*, 817–827.
- Oppenheim, D.E., Roberts, S.J., Clarke, S.L., Filler, R., Lewis, J.M., Tigelaar, R.E., Girardi, M., and Hayday, A.C. (2005). Sustained localized expression of ligand for the activating NKG2D receptor impairs natural cytotoxicity in vivo and reduces tumor immunosurveillance. *Nat. Immunol.* *6*, 928–937.
- Orange, J.S., and Biron, C.A. (1996). Characterization of early IL-12, IFN- α beta, and TNF effects on antiviral state and NK cell responses during murine cytomegalovirus infection. *J. Immunol.* *156*, 4746–4756.
- Raulet, D.H. (2003). Roles of the NKG2D immunoreceptor and its ligands. *Nat. Rev. Immunol.* *3*, 781–790.
- Robbins, S.H., Tessmer, M.S., Mikayama, T., and Brossay, L. (2004). Expansion and contraction of the NK cell compartment in response to murine cytomegalovirus infection. *J. Immunol.* *173*, 259–266.
- Saez-Borderias, A., Guma, M., Angulo, A., Bellosillo, B., Pende, D., and Lopez-Botet, M. (2006). Expression and function of NKG2D in CD4+ T cells specific for human cytomegalovirus. *Eur. J. Immunol.* *36*, 3198–3206.
- Sjolín, H., Tomasello, E., Mousavi-Jazi, M., Bartolazzi, A., Karre, K., Vivier, E., and Cerboni, C. (2002). Pivotal role of KARAP/DAP12 adaptor molecule in the natural killer cell-mediated resistance to murine cytomegalovirus infection. *J. Exp. Med.* *195*, 825–834.
- Smith, H.R., Heusel, J.W., Mehta, I.K., Kim, S., Dorner, B.G., Naidenko, O.V., Iizuka, K., Furukawa, H., Beckman, D.L., Pingel, J.T., et al. (2002). Recognition of a virus-encoded ligand by a natural killer cell activation receptor. *Proc. Natl. Acad. Sci. USA* *99*, 8826–8831.
- Tomasello, E., Desmoulin, P.O., Chemin, K., Guia, S., Cremer, H., Ortaldo, J., Love, P., Kaiserlian, D., and Vivier, E. (2000). Combined natural killer cell and

- dendritic cell functional deficiency in KARAP/DAP12 loss-of-function mutant mice. *Immunity* 13, 355–364.
- Wiemann, K., Mittrucker, H.W., Feger, U., Welte, S.A., Yokoyama, W.M., Spies, T., Rammensee, H.G., and Steinle, A. (2005). Systemic NKG2D down-regulation impairs NK and CD8 T cell responses in vivo. *J. Immunol.* 175, 720–729.
- Wu, J., Song, Y., Bakker, A.B., Bauer, S., Spies, T., Lanier, L.L., and Phillips, J.H. (1999). An activating immunoreceptor complex formed by NKG2D and DAP10. *Science* 285, 730–732.
- Wu, J., Cherwinski, H., Spies, T., Phillips, J.H., and Lanier, L.L. (2000). DAP10 and DAP12 form distinct, but functionally cooperative, receptor complexes in natural killer cells. *J. Exp. Med.* 192, 1059–1068.
- Zompi, S., Hamerman, J.A., Ogasawara, K., Schweighoffer, E., Tybulewicz, V.L., Di Santo, J.P., Lanier, L.L., and Colucci, F. (2003). NKG2D triggers cytotoxicity in mouse NK cells lacking DAP12 or Syk family kinases. *Nat. Immunol.* 4, 565–572.